Applied Physics Letters

Characterizing nonlocal dispersion compensation in deployed telecommunications fiber

Cite as: Appl. Phys. Lett. **114**, 131106 (2019); https://doi.org/10.1063/1.5088830
Submitted: 14 January 2019 . Accepted: 27 February 2019 . Published Online: 04 April 2019

James A. Grieve, Yicheng Shi, Hou Shun Poh, Christian Kurtsiefer, and Alexander Ling

Applied Physics Letters ARTICLE scitation.org/journal/apl

Characterizing nonlocal dispersion compensation in deployed telecommunications fiber

Cite as: Appl. Phys. Lett. **114**, 131106 (2019); doi: 10.1063/1.5088830
Submitted: 14 January 2019 · Accepted: 27 February 2019 ·
Published Online: 4 April 2019

James A. Grieve,[1,a)] Yicheng Shi,[1] Hou Shun Poh,[1] Christian Kurtsiefer,[1,2] and Alexander Ling[1,2]

AFFILIATIONS

[1]Centre for Quantum Technologies, 3 Science Drive 2, National University of Singapore, 117543 Singapore
[2]Department of Physics, National University of Singapore, Blk S12, 2 Science Drive 3, 117551 Singapore

[a)]Electronic mail: james.grieve@nus.edu.sg

ABSTRACT

Propagation of broadband photon pairs over deployed telecommunication fibers is used to achieve nonlocal dispersion compensation without the deliberate introduction of negative dispersion. This is made possible by exploiting time-energy entanglement and the positive and negative dispersive properties of the fiber. We demonstrate the preservation of photon timing correlations after transmission over two multi-segment 10 km spans of deployed fiber and up to 80 km of laboratory-based fiber.

Correlated photon pairs created via spontaneous parametric downconversion (SPDC) are a core component in entanglement based quantum key distribution (QKD)[1–10] and may also be used as a resource for clock synchronization.[11,12] Photon pairs produced by this mechanism are created within a short time window [typically 10 fs to 100 fs (Ref. 13)] and so share a high degree of temporal correlation. As the SPDC process is inherently broadband, fiber chromatic dispersion can obscure these timing correlations. In practical terms, this reduces the precision with which remotely detected photon pairs can be identified, increasing the rate of spurious "background" events. This may negatively impact QKD error rates[14] and reduce the performance of clock synchronization protocols. For this reason, photon pair sources are often filtered spectrally prior to use in optical fiber links, reducing the throughput of the entire system.[15,16]

Management and engineering of dispersion are routine tasks in fiber optic communications.[17,18] In 1992, Franson[19] showed that photon pairs entangled in the time-energy basis could experience nonlocal compensation of chromatic dispersion, provided that the photons propagate through media with opposite dispersion coefficients. This is a direct consequence of quantum correlations and therefore impossible to replicate with classical light—a concept later expanded by Wasak *et al.*,[20] who proposed the preservation of tight timing correlations in the presence of dispersive transmission as an entanglement witness. Beyond chromatic dispersion, related mechanisms such as polarization mode dispersion[21] have also been studied in the context of nonlocal compensation effects.[22]

The nonlocal compensation of chromatic dispersion has been observed in the visible and near-infrared spectral range by using dispersive elements such as prisms and gratings.[13,23–25] However, both negative and positive dispersion regions are available in all single-mode optical fibers.[26] Most deployed telecommunication fibers exhibit this behaviour around the zero dispersion wavelength close to the 1310 nm "O-band,"[18] with the location of this region specified by International Telecommunications Union standards (*ITU-T G.652*[27]).

Nonlocal dispersion compensation using the properties of a *single* optical fiber was first observed in measurements of fiber dispersion using SPDC photons[28] and was applied to QKD field tests[29] and entanglement distribution.[30] These experiments utilized a tunable source of SPDC photons to generate wavelengths that would experience dispersion compensation in two continuous spans of deployed telecommunication fiber with lengths up to 9.3 km. These early experiments illustrate the potential for nonlocal dispersion compensation to increase the signal-to-noise ratio of a quantum channel, with a recent theoretical treatment[14] also finding merit in this approach.

In this paper, we show that photon pairs which broadly degenerate at the approximate location of the zero dispersion wavelength can exhibit nonlocal dispersion compensation in standard, multi-segment telecommunication fiber. This scheme does not require specialized dispersive elements, measurement of the precise fiber characteristics, or tuning of the emission spectrum.

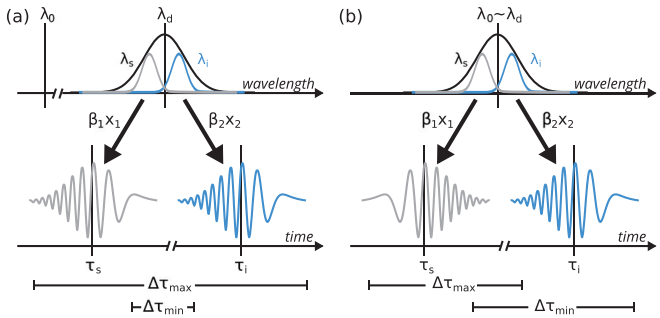

FIG. 1. Mechanism of nonlocal dispersion compensation. (a) Time-energy entangled photons are produced about the degenerate wavelength λ_d, far away from the zero dispersion wavelength λ_0 of the fiber. Signal and idler photons (λ_s, λ_i) propagate over fibers of length x_1 and x_2 and are dispersed by $\beta_1 x_1$ and $\beta_2 x_2$. In this spectral range, the dispersion coefficients β_1 and β_2 have the same sign. In the time domain, dispersed photons are represented by their electric field, with their centres denoted τ_s and τ_i. The width of the pairwise timing correlations will be related to the difference between the minimum and maximum possible delays $\Delta\tau_{min}$ and $\Delta\tau_{max}$ and we note that the anticorrelation of the photons in the wavelength maximises this discrepancy. (b) Photon pairs with $\lambda_d \sim \lambda_0$ undergo opposite dispersion. In this case, the anticorrelation in wavelength leads to a positive correlation in the observed delay, minimizing $\Delta\tau_{max} - \Delta\tau_{min}$.

Nonlocal dispersion compensation can be understood by considering the energy anticorrelation of an entangled photon pair and dispersion on the individual photon wavepackets. For positive dispersion, higher energy (shorter wavelength) components of a light pulse travel faster, while lower energy components lag behind.[31] This leads to a "chirp." The minimum and maximum delay (τ_{min} and τ_{max}) between the detection of the two photons from a pair determine the spread in observed timing correlations [Fig. 1(a)]. For opposite dispersion coefficients [Fig. 1(b)], the chirp imparted on one of the photons is reversed, and the resulting fast-fast/slow-slow correlations minimize the spread in propagation times.

The width σ of the timing distribution is related to the sum of the dispersion along the two paths ($\beta_1 x_1$ and $\beta_2 x_2$ for photons 1 and 2, respectively)[19]

$$\sigma^2 = \frac{(\beta_1 x_1 + \beta_2 x_2)^2}{2\sigma_0^2}, \tag{1}$$

where σ_0 is the coherence time of the photons, and x_1 and x_2 are the propagation distances. If the dispersion coefficients β_1 and β_2 have the opposite sign, dispersion can be at least partially compensated. For $\beta_1 x_1 = -\beta_2 x_2$, the compensation is perfect.[19]

Figure 2 shows a schematic of the experimental setup. A photon pair source is connected to two remote nodes by optical fiber. At the nodes, arrival times of single photons are recorded with respect to a local clock. Due to the timing correlation of the photon pairs, detection times $\{t_i\}$ and $\{t_j\}$ at nodes A and B are correlated. As photon pairs are created at random time intervals, their detection results in a random set of arrival times at each node. These are processed into sets of delays (d_a and d_b) such that

$$d_a(t) = \sum_i \delta(t - t_i); \quad d_b(t) = \sum_j \delta(t - t_j), \tag{2}$$

with their cross correlation c(τ)

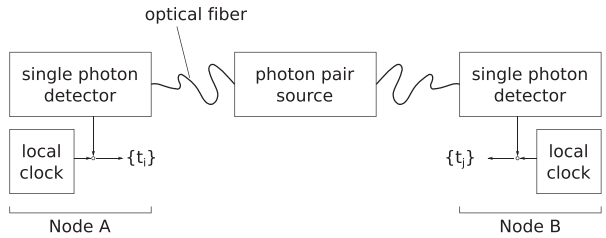

FIG. 2. A schematic of the experimental setup. Time correlated photon pairs are generated by Type-0 spontaneous parametric downconversion. The pairs are separated, routed to two nodes via single mode optical fiber, and detected by InGaAs avalanche photodiodes. Detection times are recorded with respect to a local clock.

$$c(\tau) = \int d_a(t) d_b(t + \tau) dt. \tag{3}$$

This cross correlation will exhibit a peak at a delay τ corresponding to the relative time of flight of the single photons. The identification of this peak allows the pairing of the corresponding detection events.[6] In several entanglement-based quantum key distribution systems,[4,6] the presence of significant propagation losses along with a degree of background noise makes minimizing the width of this peak an important consideration.[32]

Our photon pair source is based on Type-0 SPDC in a periodically poled crystal of potassium titanyl phosphate (PPKTP, Raicol) pumped by a grating stabilized laser diode at 658 nm (Ondax). The resulting photon pairs are degenerate at 1316 nm, close to the zero dispersion wavelength in the most common single-mode telecommunication fibers,[27] with emission sufficiently broad to span a region on either side of this wavelength (see Fig. 3). Signal and idler photons are efficiently separated using a wavelength division demultiplexer and routed to either a deployed fiber link or a bank of lab-based fibers. After propagation and dispersion, we detect the photons using commercially available InGaAs avalanche photodiodes (APDs) operated in the Geiger mode and record arrival times using timestamping modules.

There is an intrinsic uncertainty in the delay between the detection of a photon and the emission of a macroscopic electrical signal. For avalanche photodiodes, this jitter is usually on the order of hundreds of picoseconds,[33,34] while for superconducting nanowire sensors, it can be as little as tens of picoseconds.[35] This uncertainty along with the resolution of timestamping electronics provides a lower bound to the width of correlation $c(\tau)$. The InGaAs APDs used in our work exhibit a jitter of 87 ps and 110 ps.

To probe the interaction of photon pairs with the dispersive properties of optical fiber, we transmit photons through several lengths of fiber from 1 km to 10 km, cut from the same piece in order to maintain similar zero dispersion wavelengths. Figure 4 shows the width of $c(\tau)$ for the asymmetric case of one photon detected directly, while the other is first dispersed by an optical fiber. An approximately linear relationship is observed between the propagation distance and the correlation width, with a gradient of 167 ps km^{-1}. We also investigate the symmetric case where both photons are transmitted over the same fiber, before being separated and detected. In the symmetric case, dispersion is reduced to 18 ps km^{-1}. This reduction is in agreement with Eq. (1), consistent with $\beta_1 \sim -\beta_2$. While perfect compensation could be achieved by tailoring the degenerate wavelength λ_d to λ_0 of the

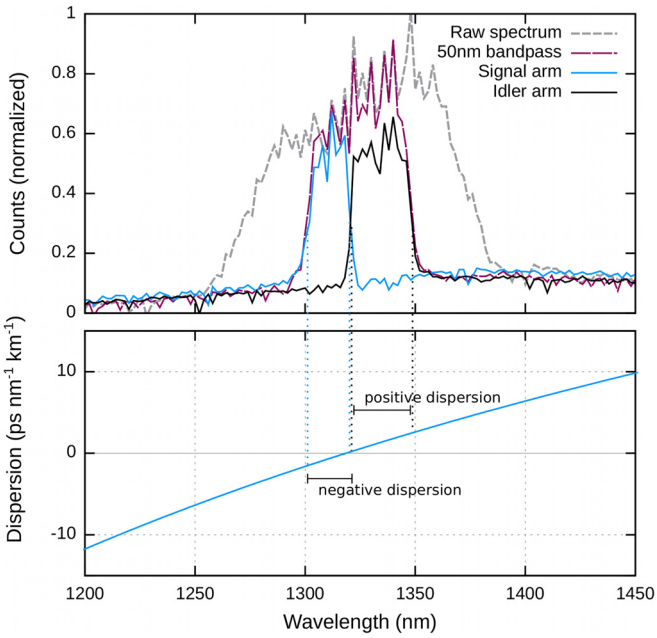

FIG. 3. Spectrum of correlated photons in this experiment. Photon pairs are degenerate around 1316 nm. In a 50 nm window defined by a bandpass filter, signal and idler photons are separated by a wavelength division demultiplexer with an edge at approximately 1316 nm. The bottom panel shows the dispersion of the popular SMF-28e (Corning[36]), a fiber conforming to the ITU-T G.652 standard.[27] Dispersion is shown for a zero dispersion wavelength (λ_0) of 1316 nm, compatible with the specified range (1302 nm to 1322 nm). Signal and idler photons propagating in this fiber will experience negative and positive dispersion.

specific fiber, this is impractical in deployed networks comprising fibers with different λ_0.

We carry out the symmetric measurement for longer fibers, with correlation signals shown in Fig. 5. These fibers are composed of several segments connected in series, with the longest (80 km) made up of three segments (10, 20, and 50 km). We no longer observe the linear

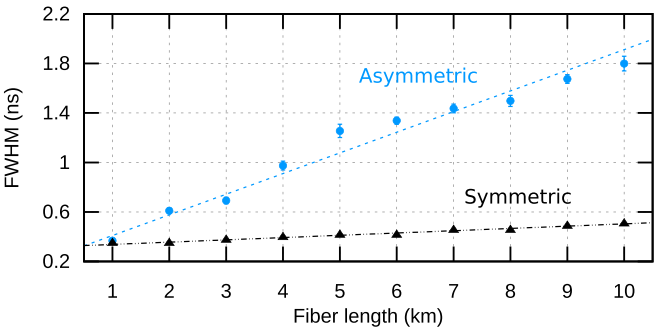

FIG. 4. Autocorrelation width (FWHM) for photon pairs after propagation through various lengths of SMF-28e optical fiber. We measure the asymmetric case of one photon detected immediately (after negligible dispersion) while the other photon is transmitted down the fiber, with the FWHM exhibiting an increase of 167 ps km^{-1}. Also shown is the symmetric case of both photons propagating in the same fiber. Here, the trend is much reduced, with a linear increase in FWHM of 18 ps km^{-1}.

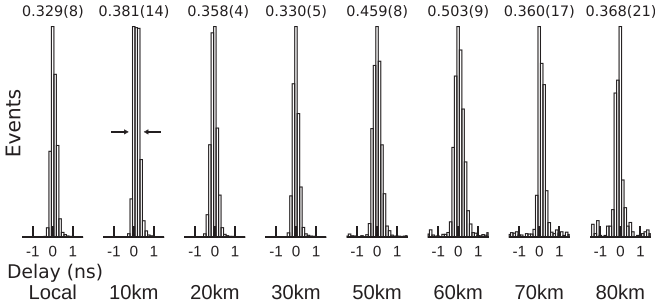

FIG. 5. Timing correlations for photon pairs transmitted through multi-segment optical fibers in a laboratory environment. The horizontal axis resolution is limited by the timestamping electronics to 125 ps, with fitted FWHM values indicated above each graph. In the minimally dispersed case ("local"), photons are routed to detectors via approximately 4 m of fiber. We observe the preservation of a high degree of timing correlation, despite transmission through up to 80 km fiber.

increase in dispersion with the fiber length (Fig. 4). However, tight timing correlations are preserved (<0.503(9) ns). We attribute small differences in the degree of dispersion compensation to variation in the exact position of the zero dispersion wavelength, which by specification may lie in a relatively wide range of 1302 nm to 1322 nm.[36]

It is interesting to note that the degree of compensation seen in the series of shorter fibers is less than for the longer spools. For example, the observed FWHM after 10 km of symmetric propagation is 0.506(7) ns, compared with 0.381(14) ns (Fig. 5). This observation again implies variation in the location of λ_0 and suggests that with a sufficiently broadband source, significant compensation is possible without tuning λ_d.

To test this mechanism in an operationally useful context, we transmit photons through two separate 10 km spans of deployed telecommunication fiber. An optical time domain reflectometer (OTDR) measurement for one fiber is shown in Fig. 6(a), revealing at least five segments. From our previous observations, we do not expect these segments to exhibit identical zero dispersion wavelengths. Measured $c(\tau)$ histograms for one photon transmitted and one detected locally and for both photons transmitted are shown in Figs. 6(b) and 6(c). With only one photon transmitted, chromatic dispersion results in a coincidence distribution with a FWHM of 1.938(47) ns. When both photons are transmitted over separate fibers, we observe a distribution with a FWHM of 0.258(7) ns.

Laboratory and field test measurements unambiguously demonstrate that photon pairs with appropriately engineered spectral properties can experience self-compensation of dispersion in conventional telecommunication fiber networks. This is despite the presence of a range of zero dispersion wavelengths and accomplished without the requirement of source tuning. This capability paves the way for the use of broad spectrum entangled light sources for quantum key distribution and other forms of quantum communication. The use of the intrinsic anomalous dispersion available in standard telecommunication fiber can minimize or even remove the need for specialized dispersion-compensating apparatus. The trade-off of operating in the O-band (where attenuation losses are higher than in the more commonly used C-band) will be acceptable for many use cases, particularly for metropolitan areas with the substantial existing fiber infrastructure.

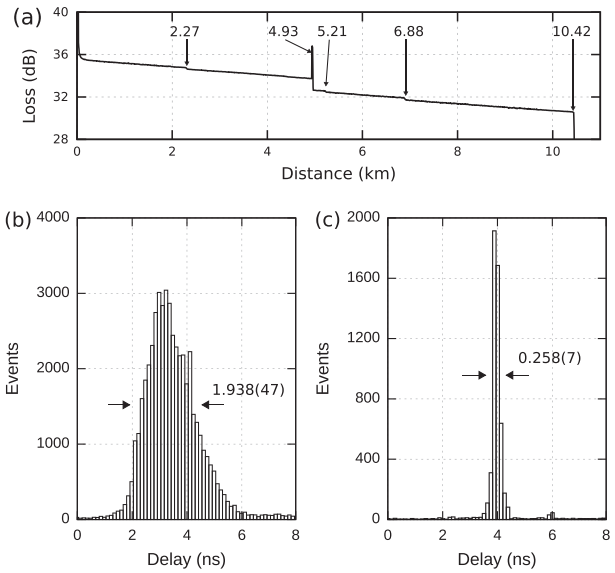

FIG. 6. Measurements of photon pairs propagating in deployed telecommunication fiber. (a) 1310 nm OTDR measurement of one fiber span, showing a length of 10.42 km. At least four splices are observed. (b) and (c) Cross correlation histograms; (b) one photon is detected locally while the other propagates over a deployed fiber prior to detection; (c) both photons travel through separate deployed fibers. Fiber spans formed two loops, beginning and ending in the lab. Photons were detected using InGaAs avalanche photodiodes and timestamped at a nominal resolution of 125 ps (the small features observed at 4 ns (b) and 6 ns (c) are due to an artifact of the data acquisition). Delays of 52 230 and 128 ns have been subtracted from (b) and (c), respectively, for ease of comparison.

This research was supported by the National Research Foundation, Prime Minister's Office, Singapore under its Corporate Laboratory@University Scheme, National University of Singapore, and Singapore Telecommunications Ltd.

The authors thank Amelia Tan Peiyu and the Singtel fiber team for facilitating our deployed fiber tests.

REFERENCES

[1] T. Jennewein, C. Simon, G. Weihs, H. Weinfurter, and A. Zeilinger, Phys. Rev. Lett. **84**, 4729 (2000); e-print arXiv:9912117 [quant-ph].
[2] G. Ribordy, J. Brendel, J. D. Gautier, N. Gisin, and H. Zbinden, Phys. Rev. A **63**, 012309 (2001); e-print arXiv:0008039v2 [arXiv:quant-ph].
[3] A. Poppe, A. Fedrizzi, T. Loruenser, O. Maurhardt, R. Ursin, H. R. Boehm, M. Peev, M. Suda, C. Kurtsiefer, H. Weinfurter, T. Jennewein, and A. Zeilinger, Quantum Opt. **12**, 3865 (2004); e-print arXiv:0404115 [quant-ph].
[4] R. Ursin, F. Tiefenbacher, T. Schmitt-Manderbach, H. Weier, T. Scheidl, M. Lindenthal, B. Blauensteiner, T. Jennewein, J. Perdigues, P. Trojek, B. Ömer, M. Fürst, M. Meyenburg, J. Rarity, Z. Sodnik, C. Barbieri, H. Weinfurter, and A. Zeilinger, Nat. Phys. **3**, 481 (2007); e-print arXiv:1203.0980.
[5] H. Hübel, M. R. Vanner, T. Lederer, B. Blauensteiner, T. Lorünser, A. Poppe, and A. Zeilinger, Opt. Express **15**, 7853 (2007); e-print arXiv:0801.3620.
[6] I. Marcikic, A. Lamas-Linares, and C. Kurtsiefer, Appl. Phys. Lett. **89**, 101122 (2006); e-print arXiv:0606072 [quant-ph].
[7] T. Honjo, S. W. Nam, H. Takesue, Q. Zhang, H. Kamada, Y. Nishida, O. Tadanaga, M. Asobe, B. Baek, R. Hadfield, S. Miki, M. Fujiwara, M. Sasaki, Z. Wang, K. Inoue, and Y. Yamamoto, Opt. Express **16**, 19118 (2008).
[8] M. P. Peloso, I. Gerhardt, C. Ho, A. Lamas-Linares, and C. Kurtsiefer, New J. Phys. **11**, 045007 (2009); e-print arXiv:0812.1880.
[9] T. Inagaki, N. Matsuda, O. Tadanaga, M. Asobe, and H. Takesue, Opt. Express **21**, 23241 (2013); e-print arXiv:1310.5473.
[10] J. Yin, Y. Cao, Y.-H. Li, J.-G. Ren, S.-K. Liao, L. Zhang, W.-Q. Cai, W.-Y. Liu, B. Li, H. Dai, M. Li, Y.-M. Huang, L. Deng, L. Li, Q. Zhang, N.-L. Liu, Y.-A. Chen, C.-Y. Lu, R. Shu, C.-Z. Peng, J.-Y. Wang, and J.-W. Pan, Phys. Rev. Lett. **119**(20), 200501 (2017).
[11] A. Valencia, G. Scarcelli, and Y. Shih, Appl. Phys. Lett. **85**, 2655 (2004); e-print arXiv:0407204 [quant-ph].
[12] C. Ho, A. Lamas-Linares, and C. Kurtsiefer, New J. Phys. **11**, 045011 (2009); e-print arXiv:0901.3203.
[13] K. A. O'Donnell, Phys. Rev. Lett. **106**, 063601 (2011); e-print arXiv:1103.0532.
[14] K. Sedziak, M. Lasota, and P. Kolenderski, Optica **4**(1), 84–89 (2017); e-print arXiv:1607.01783.
[15] S. Fasel, N. Gisin, G. Ribordy, and H. Zbinden, Eur. Phys. J. D **30**, 143 (2004); e-print arXiv:0403144v1 [arXiv:quant-ph].
[16] S. Wengerowsky, S. K. Joshi, F. Steinlechner, J. R. Zichi, S. Dobrovolskiy, R. van der Molen, J. W. Los, V. Zwiller, M. A. Versteegh, A. Mura *et al.*, preprint arXiv:1803.00583 (2018).
[17] G. Keiser, "Optical fiber communications," in *Wiley Encyclopedia of Telecommunications*, Wiley Encyclopedia of Telecommunications (Wiley, 2003).
[18] B. J. Ainslie and C. R. Day, J. Lightwave Technol. **LT-4**, 967–979 (1986).
[19] J. D. Franson, Phys. Rev. A **45**, 3126 (1992).
[20] T. Wasak, P. Szańkowski, W. Wasilewski, and K. Banaszek, Phys. Rev. A **82**, 052120 (2010); e-print arXiv:1006.5854.
[21] M. Brodsky, E. C. George, C. Antonelli, and M. Shtaif, Opt. Lett. **36**, 43 (2011).
[22] M. Shtaif, C. Antonelli, and M. Brodsky, Opt. Express **19**, 1728 (2011).
[23] A. M. Steinberg, P. G. Kwiat, and R. Y. Chiao, Phys. Rev. Lett. **68**, 2421 (1992); e-print arXiv:0000135489.
[24] S. Y. Baek, Y. W. Cho, and Y. H. Kim, in 2011 IEEE Photonics Society Summer Topical Meeting Series 17 (2011), p. 35; e-print arXiv:0811.2035.
[25] J. P. W. Maclean, J. M. Donohue, and K. J. Resch, Phys. Rev. Lett. **120**, 053601 (2018); e-print arXiv:1710.11541.
[26] L. G. Cohen and C. Lin, Appl. Opt. **16**, 3136 (1977).
[27] *Characteristics of a Single-Mode Optical Fibre and Cable*, iTU-T G.652 Version 9.0 (International Telecommunications Union, Geneva, CH, 2016).
[28] J. Brendel, H. Zbinden, and N. Gisin, Opt. Commun. **151**, 35 (1998).
[29] W. Tittel, J. Brendel, H. Zbinden, and N. Gisin, Phys. Rev. Lett. **81**, 3563 (1998).
[30] W. Tittel, J. Brendel, N. Gisin, and H. Zbinden, Phys. Rev. A **59**, 4150 (1999); e-print arXiv:9809025 [quant-ph].
[31] B. E. Saleh, M. C. Teich, and B. E. Saleh, *Fundamentals of Photonics* (Wiley, New York, 1991), Vol. 22.
[32] E. Diamanti, H.-K. Lo, B. Qi, and Z. Yuan, NPJ Quantum Inf. **2**, 16025 (2016); e-print arXiv:1606.05853.
[33] T. Lunghi, C. Barreiro, O. Guinnard, R. Houlmann, X. Jiang, M. A. Itzler, and H. Zbinden, J. Mod. Opt. **59**, 1481 (2012); e-print arXiv:1204.4594v1.
[34] M. Stipcevic, D. Wang, and R. Ursin, J. Lightwave Technol. **31**, 3591 (2013).
[35] C. M. Natarajan, M. G. Tanner, and R. H. Hadfield, Supercond. Sci. Technol. **25**, 063001 (2012).
[36] *Corning SMF-28e Optical Fiber Product Information* (Corning, Inc., 2005).